https://doi.org/10.5194/egusphere-2025-3687
Preprint. Discussion started: 11 August 2025

Carbon and nitrogen allocation in montane vegetation: Understanding the impact of environmental change on ecosystem processes

Bibhasvata Dasgupta[1,2], Prasanta Sanyal[1,3]

[1]Department of Earth Sciences, Indian Institute of Science Education and Research Kolkata, Mohanpur 741246, India.

[2]Department of Physics, Institute for Marine and Atmospheric research Utrecht, Utrecht University, Utrecht, The Netherlands

[3]Centre for Climate and Environmental Studies, Indian Institute of Science Education and Research Kolkata, Mohanpur, India

Correspondence to: Bibhasvata Dasgupta (bdasgupta03@gmail.com)

Abstract. Mountain forests, comprising nearly 20% of the world's forest cover, are among the most ecologically fragile ecosystems due to their strong topographic and climate sensitivity. Understanding how climate influences these ecosystems requires examining the allocation of key nutrients like carbon (C) and nitrogen (N). We investigated foliar C and N allocation in the Himalayan vegetation by sampling 141 leaf samples from 14 species across three climatically different transects spanning 1,900–5,200 m. The mean total nitrogen (TN) was 6.6 ± 4.5 %, with Juniperus and Abies exhibiting the highest TN (8.3 %) and grasses the lowest (1.6 %). Foliar $\delta^{15}N$ ranged from +2.1 ‰ in Juniperus to +8.9 ‰ in grasses, varying inversely with TN. Total organic carbon (TOC) averaged 37.5 ± 6.2 %, peaking in Juniperus (40.6 %) and lowest in Abies (34.2 %). Foliar $\delta^{13}C$ in C_3 species clustered near –27 ‰, while C_4 grasses reached –13.4 ‰. In the Central Himalaya, Juniperus maintained high TN and TOC at altitude, whereas in the West, Rhododendron had elevated TN and TOC relative to other genera. Statistical analyses showed that warmer growing seasons strongly reduced TN in Abies and Rhododendron, and wetter conditions increased $\delta^{13}C$ in Abies and TN in Pinus. Clustering of $\delta^{13}C$ and TN effectively distinguished mycorrhizal types, with arbuscular-associated grasses displaying higher $\delta^{13}C$ and lower TN than ectomycorrhizal and ericoid-associated taxa. Geostatistical modelling produced a dual-isotope map revealing "arid hotspots"

https://doi.org/10.5194/egusphere-2025-3687
Preprint. Discussion started: 11 August 2025

(high $\delta^{15}N$ and $\delta^{13}C$, low TN) in dry western valleys and "humid cold spots" (low $\delta^{15}N$ and $\delta^{13}C$, high TN and TOC) in moist eastern slopes. These findings demonstrate that steep precipitation and temperature gradients drive N much more than C in Himalayan plants, underscore the tight coupling of C and N, and identify areas most sensitive to climate-induced shifts in nutrient allocation.

1 Introduction

The cycling of carbon (C) in plant communities encompasses photosynthesis, respiration, decomposition, and nutrient uptake—processes that govern productivity, biomass accumulation, and C sequestration (Pidwirny 2006; Metcalfe et al. 2011). Nitrogen (N) is likewise essential, as a constituent of Rubisco and other key enzymes driving photosynthesis; its cycling through fixation, nitrification, denitrification, and mineralisation underpins plant N-acquisition strategies and responses to environmental change (Hart et al. 1994; Raines 2003; Kraiser et al. 2011).

A complex interplay of genetic, physiological, and environmental factors governs N allocation in plants. Genetically, plants regulate N distribution among organs (leaves, stems, roots) in response to N availability (Kalcsits et al. 2014). Physiological processes such as photosynthesis and protein synthesis drive N allocation to leaves, while respiration promotes root allocation (Evans & Clarke, 2019). Equally, C allocation responds to variables like light, CO_2, water availability, temperature, and soil properties (Ericsson et al. 1996). Moisture stress, for instance, can alter C partitioning and photosynthetic capacity (Centritto 2005), and increased C allocation to leaves supports amino-acid and protein synthesis (Li et al. 2020). Because C and N cycles are tightly linked, foliar C and N pools vary together along environmental gradients (Ericsson et al. 1996; Li et al. 2020).

Montane ecosystems, characterised by steep climatic gradients, short growing seasons, and nutrient-poor soils, are particularly sensitive to these interactions. Growing-season temperature (GST) and precipitation (GSP) influence both C and N allocation, and climate change is expected to disrupt established C–N linkages. Warming may accelerate soil organic matter mineralisation, increasing N

https://doi.org/10.5194/egusphere-2025-3687
Preprint. Discussion started: 11 August 2025

availability but also enhancing losses via leaching and gas emissions (Okello et al. 2022; Cregger et al. 2014). This can enrich $\delta^{15}N$ in soils and leaves (Ariz et al. 2015; Luo et al. 2018). Warmer, drier conditions can reduce stomatal conductance, raising foliar $\delta^{13}C$ (Liu & Wang 2010), while precipitation shifts may enhance or suppress TN depending on local factors (Peri et al. 2012; Luo et al. 2018). At the ecosystem level, warming can boost net primary productivity in cold-limited forests (Gimeno et al. 2012), whereas moisture stress reduces carbon uptake and increases respiration (Morecroft et al. 1996; Salinas et al. 2021).

Despite global interest in montane C–N dynamics, high-elevation data from the Himalayas—one of Earth's steepest climatic gradients—remain sparse. By sampling 141 individuals across 14 species (gymnosperms, angiosperms, and grasses) from 1,900 to 5,200 m, we assemble one of the most comprehensive Himalayan altitudinal transects to date. The west-to-east climatology—from dry subtropical foothills to cold, moist alpine plateaus—makes the Himalayas an ideal "natural laboratory" for examining how C and N uptake respond to synchronous changes in temperature, precipitation, and mycorrhizal associations. Investigating these patterns fills a critical geographic and elevational gap and establishes a baseline for predicting how climate change will alter montane C–N interdependence, ecosystem carbon budgets, and the resilience of high-altitude vegetation.

2 Materials and Methods

Three Himalayan river catchments (Fig. 1a) were sampled between the years 2019 and 2021 with each transect being sampled during the winter-spring months of the respective year: Karnali Basin (Western Himalaya) measuring an area of 22,685 km^2 and relief of 7996 m, sampled from Nepalganj (1900 m) to Hilsa and Mugu (4200 m); Annapurna Basin (Central Himalaya), spanning an area of 4792 km^2 and relief of 7727 m, sampled from Besisahar (2000 m) to Muktinath (4800 m); and Kosi Basin (Eastern Himalaya) stretches across an area of 4065 km^2 and relief of 8255 m, sampled from Lukla (2600 m) to Gorakshep (5200 m). Climatologically, the three transects are distinct, with a dry-to-wet and hot-to-cold gradient between the west and east (Supplementary Fig. S1). From the three transects, 141

https://doi.org/10.5194/egusphere-2025-3687
Preprint. Discussion started: 11 August 2025

Himalayan plant individuals have been sampled, comprising 14 species and 5 genera (Fig. 1b and 1c). There are 46 angiosperms, 79 gymnosperms and 10 grass samples. Three mature leaves of each plant individual were collected using nitrile gloves from areas without human disturbance.

Leaf samples were washed using 0.5N Hydrochloric acid and rinsed with distilled water for neutralisation (Basu et al., 2015). The samples were oven-dried at 45°C. Dried and powdered samples were analysed stable isotope laboratory at the Indian Institute of Science Education and Research Kolkata (IISER-K) for $\delta^{13}C$ and $\delta^{15}N$ using Flash 2000 Elemental Analyzer (EA) coupled with V Plus isotope ratio mass spectrometer (IRMS) with the help of the Conflo IV interface (Samantaray and Sanyal, 2022). The reproducibility check was done by analysing repetitive samples, CH-3 cellulose ($\delta^{13}C$= –24.6 ‰ ± 0.07 ‰), Caffeine ($\delta^{13}C$= –26.5 ‰ ± 0.10 ‰; $\delta^{15}N$= –1.10 ‰ ± 0.05 ‰), Urea ($\delta^{13}C$= –26.7 ‰ ± 0.04 ‰; $\delta^{15}N$= –1.10‰ ± 0.03 ‰) and internal laboratory standard (Motijhil: $\delta^{13}C$ = –23.8 ‰ ± 0.2 ‰). The $\delta^{13}C$ values are reported with respect to Vienna Pee Dee Belemnite (VPDB)(Coplen, 1996) and $\delta^{15}N$ values with respect to atmospheric N (Mariotti, 1983). The international standards used for N are ammonium sulphate and caffeine. Acetanilide and nicotinamide were used to generate calibration curves to calculate the TOC (%) and TN (%) concentrations in the samples. The calibration curves are TOC = 0.0166*Area − 0.1282 (R^2 = 0.99) and TN = 0.000495*Area + 0.215 (R^2 = 0.97).

https://doi.org/10.5194/egusphere-2025-3687
Preprint. Discussion started: 11 August 2025

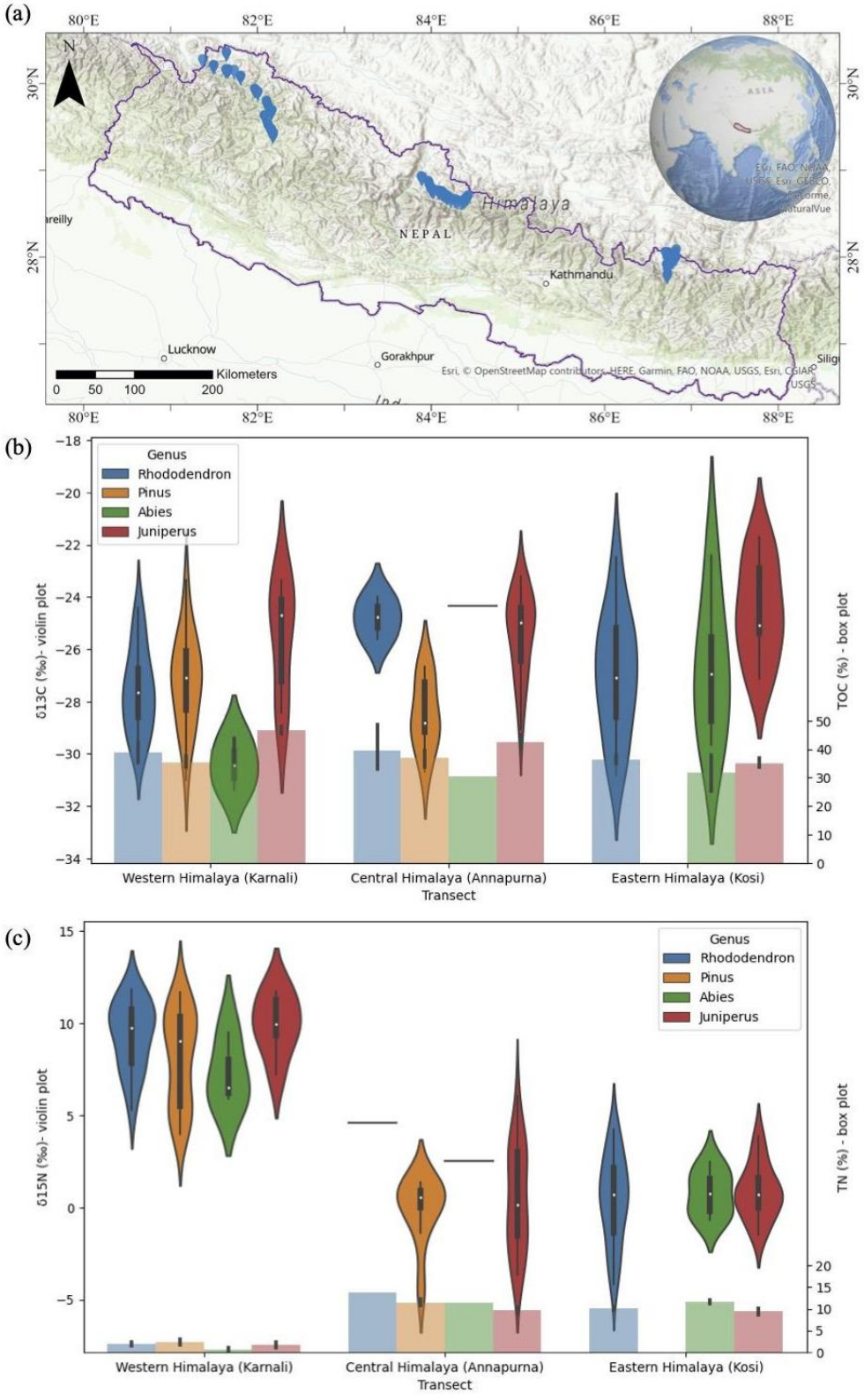

https://doi.org/10.5194/egusphere-2025-3687
Preprint. Discussion started: 11 August 2025

Figure 1: Study area map showing sampled locations in blue markers (a); Distribution of $\delta^{13}C$ values and TOC across the three transects (b); Distribution of $\delta^{15}N$ values and TN across the three transects (c).

3 Results

3.1 Abundance and isotopic composition of C and N in leaves

The average TN percentage across all 141 leaf samples is 6.6 ± 4.5 %, with Juniperus and Abies both exhibiting the highest mean TN values of 8.3 %, followed by Rhododendron at 7.1 %, Pinus at 5.1 %, and grasses at 1.6 % (Supplementary Table S1). Foliar $\delta^{15}N$ values vary inversely with TN (Pearson r = –0.80), ranging from a maximum of +8.9 ‰ in grasses to a minimum of +2.1 ‰ in Juniperus. TOC averages 37.5 ± 6.2 %, peaking in Juniperus at 40.6 % and dipping in Abies at 34.2 %. Foliar $\delta^{13}C$ values range from –29.1 ‰ in C_3 grasses to –13.4 ‰ in C_4 grasses (Supplementary Table S1). Pearson correlation and R^2 values (Supplementary Table S2; Fig. S2) indicate that GSP explains 67 % of the variance in TN and $\delta^{15}N$ but less than 5 % of the variance in TOC and $\delta^{13}C$. Elevation accounts for approximately 10 % of the variance in N-related metrics (TN, $\delta^{15}N$) and essentially 0 % of the variance in C-related metrics (TOC, $\delta^{13}C$).

Within the Central Himalaya, Juniperus displays higher TN and TOC percentages than Rhododendron, Abies, and Pinus; specifically, Juniperus TN ranges from 6.5 % to 9.2 % along the transect, and TOC ranges from 38.1 % to 42.3 %. In the Western Himalaya, Rhododendron exhibits higher TN (≈ 7.4 %) and TOC (≈ 38.5 %) than other genera, while Juniperus shows moderate to lower values (TN ≈ 6.8 %; TOC ≈ 39.8 %). Grass species in Western Himalaya demonstrate TN of 0.9 %–2.3 % and TOC of 30.2 %–36.7 %, depending on whether they follow C_3 or C_4 pathways. Across both Central Himalaya and Western Himalaya transects, higher elevations (above approximately 4,000 m) correspond to increased mean TN (≈ 8.0 %) and TOC (≈ 39.5 %). Although GSP and GST also influence TN and TOC, these relationships are complex and species-dependent.

Genus-level correlation analyses reveal that $\delta^{15}N$ and TOC have significant interrelationships in Juniperus and Abies (Kendall Tau ≈ 0.50, $p < 0.01$ for each), a lesser correlation in Rhododendron ($\tau \approx$

https://doi.org/10.5194/egusphere-2025-3687
Preprint. Discussion started: 11 August 2025

0.30, p = 0.04), and no significant correlation in Pinus (p > 0.10). In grasses, $\delta^{15}N$ and TOC are strongly but negatively correlated (Pearson r = –0.50, p < 0.01). No significant relationship exists between $\delta^{13}C$ and $\delta^{15}N$ values across most genera, with the exception of Abies (Pearson r = 0.65, p < 0.001).

3.2 Relationship of GSP and GST with C and N allocation in Himalayan plants

Linear regression analyses quantify how GST and GSP relate to foliar C and N metrics within each genus. In Abies, GST versus TN yields Pearson r = –0.93 and R^2 = 0.87, while GSP versus $\delta^{13}C$ produces r = 0.79 and R^2 = 0.63. For Rhododendron, GST versus TN is r = –0.88 (R^2 = 0.77), and GSP versus TN is r = 0.90 (R^2 = 0.81). Juniperus shows a moderate positive relationship between GST and TOC (r = 0.60, R^2 = 0.36). In Pinus, GSP versus TN yields r = 0.92 and R^2 = 0.84. All regression scores and scatterplots appear in Supplementary Figure S2.

3.3 Evaluation of isotope-abundance clustering against Mycorrhizal association

In the Himalayan dataset, the mycorrhizal associations observed are Endomycorrhizal, Ericoid, Ectomycorrhizal, and Arbuscular mycorrhiza (Singh and Singh, 2008). We evaluate the linkage between the measured C and N variables on the mycorrhizal associations via clustering analysis. Clustering is a technique for identifying natural groupings within data, which can help uncover hidden patterns or relationships. We ran K-means (optimal_k) on all pairs of [TOC, $\delta^{13}C$, TN, $\delta^{15}N$, C/N] after standardisation, then evaluated each model's Adjusted Rand Index against known mycorrhizal types. The $\delta^{13}C$–TN combination yielded the highest discriminant accuracy (Table 1; Fig. 2). K-Means aims to group data points into clusters so that data points within the same cluster are similar (Python code in Supplementary I). Clustering accuracy (Shahapure and Nicholas, 2020; Santos and Embrechts, 2009) was used as a metric to assess the effectiveness of $\delta^{13}C$ and TN in distinguishing between different mycorrhizal associations compared to other pairs (Table 1; Fig. 2). The $\delta^{13}C$ values provide insights into photosynthetic associations of plant type and mycorrhizae, while TN reflects the overall N content sourced from microbial N-fixation.

https://doi.org/10.5194/egusphere-2025-3687
Preprint. Discussion started: 11 August 2025

Table 1: Evaluate clustering against Mycorrhizal association using Adjusted Rand Index

Feature 1	Feature 2	Silhouette Score	Adjusted Rand Index
$\delta^{13}C$ (‰)	**TN (%)**	**0.53**	**0.13**
$\delta^{13}C$ (‰)	C/N	0.47	0.12
$\delta^{13}C$ (‰)	$\delta^{15}N$ (‰)	0.43	0.11
TOC (%)	TN (%)	0.44	0.09
TOC (%)	$\delta^{15}N$ (‰)	0.40	0.08
TOC (%)	**$\delta^{13}C$ (‰)**	**0.38**	**0.07**
TN (%)	C/N	0.67	0.07
TN (%)	$\delta^{15}N$ (‰)	0.41	0.05
$\delta^{15}N$ (‰)	C/N	0.51	0.03
TOC (%)	C/N	0.38	0.02

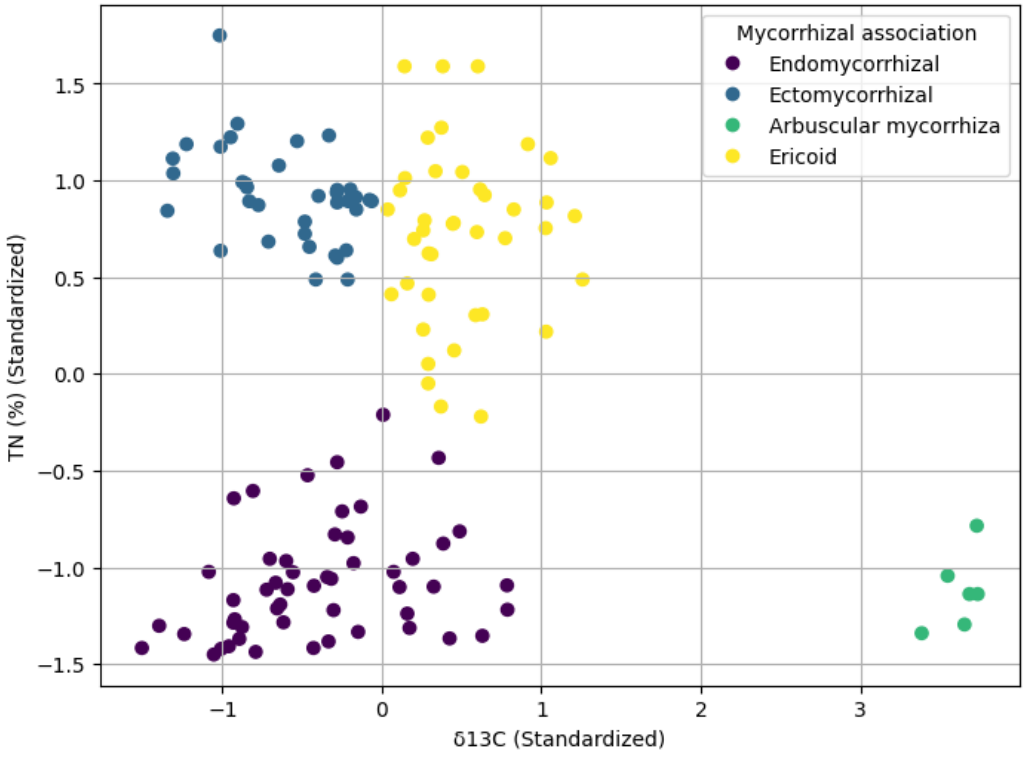

https://doi.org/10.5194/egusphere-2025-3687
Preprint. Discussion started: 11 August 2025

Figure 2: Mycorrhizae-Genera clustering results with Mycorrhizal Association Labels

3.4 Isoscape Modelling the spatial distribution of $\delta^{13}C$ and $\delta^{15}N$ values

Geostatistical models of stable isotope landscapes or isoscapes provide a complementary tool for assessing and predicting plant response to changing environmental conditions (West et al., 2010). A few key points must be followed to build isoscapes for plant leaf isotopic composition. First, we check whether the data shows any spatial correlation, without which the error propagation of the model would exceed its prediction accuracy (Li et al., 2007). For both $\delta^{13}C$ and $\delta^{15}N$ values, we performed a Moran's I spatial autocorrelation test (Supplementary Fig. 3). A Moran's Index of ≥ 0.5 and a critical value (z-score) of ≥ 1.65 or ≤ -1.65 suggests robust spatial clustering (Scott and Janikas, 2010). As per earlier observations, $\delta^{13}C$ and $\delta^{15}N$ values in plant leaves showed robust botanical and climatic controls, respectively. Therefore, the spatial autocorrelation is more significant for foliar $\delta^{15}N$ value (Moran's I = 0.93, z-score = 9.66) than for foliar $\delta^{13}C$ value (Moran's I = 0.08, z-score = 1.04). Accordingly, both isoscapes have been built.

https://doi.org/10.5194/egusphere-2025-3687
Preprint. Discussion started: 11 August 2025

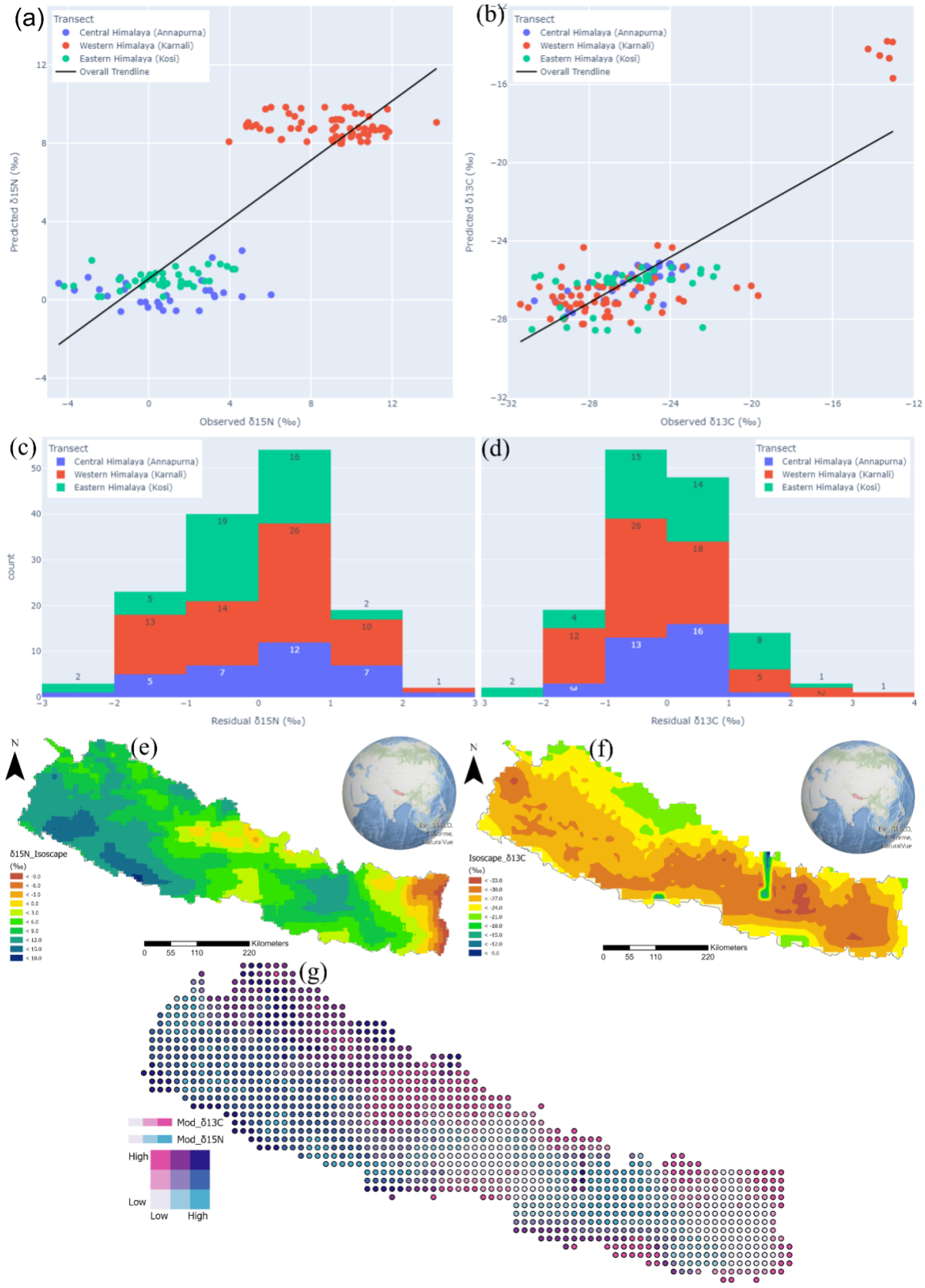

https://doi.org/10.5194/egusphere-2025-3687
Preprint. Discussion started: 11 August 2025

Figure 3: Modelling the spatial distribution of $\delta^{13}C$ and $\delta^{15}N$ values. Cross plot between observed and modelled values of (a) $\delta^{15}N$ value, (b) $\delta^{13}C$ value and their residuals (c and d), colour-coded by transect. Spatial extrapolation using Linear Multi-regression for $\delta^{15}N$ value Isoscape (e) and Ridge Regression for $\delta^{13}C$ value Isoscape (f), followed by an ArcGIS space-time cube comprising both $\delta^{13}C$ and $\delta^{15}N$ values in a dual isoscape network (g).

The foliar $\delta^{15}N$ value shows a prominent Gaussian distribution and spatial auto-correlation, and is controlled by GSP, GST, Soil microbial N (SMN) and Soil moisture content (SM). Given that no botanical controls exist, and all 4 drivers vary as a function of geography, we applied a linear multiple-regression fit to model its distribution (Hidalgo and Goodman, 2013). The equation of the fit is as follows:

$$\delta^{15}N_{plant\text{-}modelled} = 133.46 + 0.12 \times GST(K) - 0.19 \times GSP(mm) - 0.006 \times SM(kg/m^3) - 1.41 \times SMN(gN/m^2)$$

The model fit yields an accuracy of 76% (Fig. 3a), which is higher than previous global models (Amundson et al., 2003). The model residuals (observed minus predicted) exhibit a Gaussian distribution (Fig. 3c), representing a well-tuned and distributed model prediction (Hensman et al., 2015). The $\delta^{15}N$ value isoscape yields minimum residual in the central Himalayan region, possibly because this part has the highest data density. The Western Himalayas show slightly higher residuals, followed by the Eastern Himalayas.

We undertook a remote sensing approach to modelling foliar $\delta^{13}C$ values (Powell et al., 2012; Cotton et al., 2016). Given that the botanical control (C_3 and C_4) over the $\delta^{13}C$ values could be extrapolated spatially by determining the relative abundance of C_3 and C_4 plants in the study area, we employed the ISLSCP II C_4 Vegetation database hosted by NASA Earthdata (source resolution 1*1 degrees; Still et al., 2009) and downscaled it to the Himalayan region using precipitation and temperature ensemble means (model resolution 0.01*0.01 degrees). The precipitation and temperature thresholds for C_3 and C_4 partitioning were obtained from Cotton et al. (2016). For each pixel, we generated a ratio of C_3 to C_4 plant abundance, then fed this to a Ridge Regressor (Marquardt and Snee, 1975) as a categorical variable, in addition to GSP, GST, SMN, SM and Elevation. The equation of fit is as follows:

https://doi.org/10.5194/egusphere-2025-3687
Preprint. Discussion started: 11 August 2025

$$\delta^{13}C_{plant\text{-}modelled} = -210.97 + 0.16 \times GST(K) - 0.0003 \times GSP(mm) - 0.001 \times Elevation(m) + 1.29 \times SMN(gN/m^2) \pm 6.27 \times C_3/C_4$$

The model fit yields an accuracy of 64 % (Fig. 3b), which is higher than previous global models (Basu et al., 2021). The model residuals (observed minus predicted) exhibit a Gaussian distribution (Fig. 3d), suggesting a well-tuned and distributed model prediction. The $\delta^{13}C$ isoscape yields minimum residual in the central Himalayan region, possibly because this part has the highest data density. The Western Himalayas show slightly higher residuals, followed by the Eastern Himalayas. We define a Dual Isoscape as a geospatial map of 2 or more complementary isotopes, which in this case are $\delta^{13}C$ and $\delta^{15}N$. Two thematic maps (Fig. 3 e,f) are embedded onto a 4-dimensional matrix (latitude × longitude × $\delta^{13}C$ × $\delta^{15}N$). Figure 3g shows a dual isoscape for foliar $\delta^{13}C$ and $\delta^{15}N$ values overlaid on the Himalayas.

4 Discussion

N plays a pivotal role in plant development, growth, and reproduction, sourced as NH_4^+, NO_3^-, or amino acids from the soil or associated symbiotic microbes. Once acquired, N is vital for protein synthesis, with proteins serving structural and enzymatic functions within plant cells. Photosynthesis, a key biological process, relies on proteins in the Calvin cycle and thylakoid membranes, representing the majority of leaf N. The abundance of these proteins, crucial for light capture and electron transport, varies in response to growth irradiance. The forthcoming section explores the intricate relationship between C and N distribution in the montane context, emphasising the mutual controls governing these essential elements in high-altitude ecosystems.

4.1 Variability in TOC and TN

4.1.1 Observed Patterns and Climatic Controls

Multivariate analyses showed that GSP explains 67 % of TN and $\delta^{15}N$ variance but less than 5 % of TOC and $\delta^{13}C$ variance. Elevation accounts for ~ 10 % of N metrics and ~ 0 % of C metrics. Within the Central Himalaya, TN weakly declined with elevation (r = –0.25), while TOC slightly increased (r =

https://doi.org/10.5194/egusphere-2025-3687
Preprint. Discussion started: 11 August 2025

+0.20). In the Western Himalaya, neither TN nor TOC correlated significantly with elevation. In Eastern Himalaya, TOC decreased moderately with elevation ($r \approx -0.45$) while TN was uncorrelated. Grasses exhibited a steep TOC rise with elevation: C_3 grasses at 4,500 m showed TOC ≈ 37 %, versus ≈ 32 % for C_4 grasses at 2,800 m. Analysis per species indicates that higher growing-season temperatures strongly reduce TN in Abies and Rhododendron, whereas warmer conditions moderately enhance TOC in Juniperus. Increased precipitation strongly elevates $\delta^{13}C$ in Abies and TN in both Pinus and Rhododendron.

Higher TN and TOC in Central-Himalaya Rhododendron likely stem from symbiotic N fixation and leaf litter quality (Ma et al., 2020), whereas Juniperus in both Central and Eastern transects benefits from warm springs and high summer precipitation (Schickhoff, 2005; Gimeno et al., 2012). Abies and Juniperus maintain high TOC at altitude due to recalcitrant structural carbon (lignin, resins), whereas broadleaved Pinus and Rhododendron show modest TOC declines with elevation, reflecting reduced lignin and cellulose under low temperatures (Richardson, 2004; Hoch, 2007). C_3 grasses increase TOC at high elevations by augmenting hemicellulose (Morrison, 1980), while C_4 grasses allocate less structural C in warmer, drier zones. This rationale is further explored in sections 4.2 and 4.3.

4.1.2 C–N Interdependence

Our study confirms that foliar C and N are tightly coupled. Leaves with higher TN supported greater C assimilation: transects with high foliar N exhibited less negative $\delta^{13}C$ (indicating higher water-use efficiency) than N-poor sites. This matches expectations that increased N allows more photosynthetic enzymes, raising intrinsic water-use efficiency and $\delta^{13}C$. Conversely, low-N sites displayed more negative $\delta^{13}C$. However, gymnosperms (Juniperus, Abies) decoupled: their TOC remained high at altitude despite declining TN, reflecting allocation to lignin and resins regardless of N. Broadleaved species (Rhododendron) tracked TN more closely, altering TOC in step with N.

Across transects, both TN and TOC declined with elevation (1,900 m to 5,200 m), but TN fell more steeply. In Eastern Himalaya, TN remained high (≈ 8–10 %) to 4,500 m before decreasing, while TOC only slightly declined from ≈ 40 % to ≈ 34 %. In Western Himalaya, TN plummeted from ≈ 7–8 % at 2,000 m to ≈ 2–3 % at 4,200 m; TOC dipped from ≈ 39 % to ≈ 36 %. The Central Himalaya showed

https://doi.org/10.5194/egusphere-2025-3687
Preprint. Discussion started: 11 August 2025

intermediate behaviour. Thus, low-elevation plants in wetter zones accumulate proportionally more N relative to C than high-elevation plants. The stronger altitudinal TN decline ($r \approx -0.50$) versus TOC ($r \approx -0.20$) underscores the higher sensitivity of N to climate.

4.1.3 Variability in $\delta^{13}C$ and $\delta^{15}N$ Values

Foliar $\delta^{15}N$ spanned –2.3 ‰ to +8.9 ‰ (mean ≈ +3.4 ‰). In Western Himalaya's arid west, $\delta^{15}N$ peaked at +8.9 ‰ in grasses, whereas in Eastern Himalaya's humid east it averaged +0.6 ‰. These gradients reflect open versus closed N cycling: dry zones lose 14N preferentially, enriching 15N, while wet zones retain N. Foliar $\delta^{13}C$ ranged from –29.1 ‰ in C_3 grasses to –13.4 ‰ in C_4 grasses (mean ≈ –26.4 ‰ for C_3 species). Western Himalaya's water-limited sites (GSP ≈ 300–400 mm) forced stomatal closure, elevating $\delta^{13}C$ to –24 ‰; Eastern Himalaya's moist sites (GSP > 1,200 mm) allowed stomata to remain open, producing $\delta^{13}C$ near –28 ‰.

Within each transect, $\delta^{13}C$ was generally enriched with elevation in Western Himalaya ($r \approx +0.25$), was nearly flat in Central Himalaya ($r \approx +0.10$), and was slightly depleted in Eastern Himalaya ($r \approx -0.20$). $\delta^{15}N$ did not follow a linear altitudinal trend: mid-elevations often showed the lowest $\delta^{15}N$ (≤ +0.5 ‰), while some high-elevation sites exhibited elevated $\delta^{15}N$ (+2 ‰), possibly due to increased nitrification in cold, wet soils above the tree line (see section 4.3.1). These patterns contrast with many global mountains, where $\delta^{15}N$ steadily declines with altitude due to progressive N limitation (Liu & Wang, 2010; Van de Weg et al., 2009). In the Himalaya, monsoonal pulses and snowpack dynamics create a more complex $\delta^{15}N$–elevation relationship.

4.2 Biological Feedback of Himalayan Flora to Climate Change

Projected warming and altered precipitation will profoundly affect Himalayan C–N dynamics (IPCC 2023). In Eastern Himalaya's monsoon-fed zones, warming and increased rainfall may accelerate soil organic matter decomposition (Okello et al., 2022), boosting soil microbial N (SMN) and lowering $\delta^{15}N$. Foliar TN could rise by ≈ 0.2 % per 0.5 °C warming, enhancing C assimilation ($\delta^{13}C$ slightly more positive). As a result, eastern forests could increase aboveground biomass by 10–15 % over two decades, strengthening carbon sinks. Yet, if mineralisation outpaces uptake, nitrate leaching may open the N cycle,

https://doi.org/10.5194/egusphere-2025-3687
Preprint. Discussion started: 11 August 2025

raising $\delta^{15}N$ and reducing N use efficiency. Over time, higher C:N litter could slow decomposition, temporarily sequestering soil C until the ecosystem re-equilibrates. In the Central Himalaya, moderate monsoon and cold winters currently constrain decomposition. Under +2 °C warming without major precipitation changes, spring mineralisation may advance by 2–3 weeks, lowering $\delta^{15}N$ in early-flush leaves by ≈ 0.5 ‰ and boosting foliar TN by ≈ 0.5 % at 3,500 m. This could increase carbon assimilation (more negative $\delta^{13}C$) by ≈ 10 %. However, reduced snowpack may limit late-season N pulses (Miller et al., 2005). Net effect: ≈ 5 % annual C uptake increase but shifts in phenology—earlier leaf emergence and extended growing season—raising leaf area index by ≈ 8 % over a decade and risking progressive nitrogen limitation (PNL) if labile N is not replenished (Luo et al., 2004). In Western Himalaya's rain-shadow parts, a 10–15 % GSP decline by 2050, combined with +2°C warming, may intensify N limitation: foliar TN could fall by 0.5–1 % at low elevations (2,000–3,500 m), while $\delta^{15}N$ could rise by ≈ 0.8–1.0 ‰. Warming (+2°C) would also enrich $\delta^{13}C$ by ≈ 0.32 ‰, indicating greater stomatal closure. Plant communities may shift from N-limited shrubs to drought-tolerant grasses, reducing biomass and carbon stocks by ≈ 10 % over two decades; $\delta^{15}N$ enrichment will signal an increasingly open N cycle. Continued aridity could force the tree line downslope, exposing soils and releasing stored C.

Thus, climate-driven shifts in N cycling are poised to determine whether Himalayan ecosystems become stronger carbon sinks or sources. If N mineralisation and deposition keep pace with warming, eastern and central forests may incrementally increase C uptake. Conversely, if N inputs decline (especially in the west), PNL will dampen CO_2 fertilisation, slowing biomass growth. Rising litter C:N ratios will retard decomposition, causing short-term soil C gains but depleting long-term N pools. Consequently, even minor shifts in precipitation or temperature can markedly alter foliar $\delta^{15}N$ ($\delta^{15}N_{plant\text{-}modelled}$ attribute ≈ 76 % of $\delta^{15}N$ variance to climate), reshaping ecosystem C fluxes.

4.3 Availability, adaptability and mycorrhizal association - 3 aspects of montane environments to understand C/N allocation

4.3.1 Availability

N availability in montane ecosystems is highly variable and a function of in situ organic matter and nitrification processes (Weintraub et al., 2017). The Himalayan vegetation contributes to high primary

https://doi.org/10.5194/egusphere-2025-3687
Preprint. Discussion started: 11 August 2025

productivity, with plant groups such as conifers, junipers, rhododendrons, and mountain grass having diverse ways of procuring N at high altitudes. N being a limiting nutrient in many montane ecosystems, its availability can affect plant growth and productivity by limiting the rate of photosynthesis and the production of organic C compounds that are used to synthesise amino acids. Conversely, primary productivity can affect N uptake and cycling because plants take N from the soil through their roots, and the N uptake rate is influenced by the availability of nutrients, such as phosphorus and potassium (Hobbie, 1992). Thus, different soil types and associated organic matter sourced from in situ productivity can reflect varying levels of organic matter and nutrient availability. Some soils may naturally have higher organic C content but lower N content, while others may have the opposite pattern (Batjes, 1996). This difference in soil composition can influence the availability and uptake of C and N by plants, leading to an inverse relationship between TOC and TN in Abies ($r = -0.5$), Juniperus ($r = -0.4$) and Rhododendrons ($r = -0.2$). Spatial variations in TN and TOC among different transects and genera highlight the importance of local environmental conditions and plant species composition. In addition, the $\delta^{15}N$ value of plants can also vary depending on the type of nitrification processes in the soil. For example, montane ecosystems growing in high snow-cover areas undergo cryospheric processes such as photolysis of nitrate (NO_3^-) on snow surfaces, which leads to the deposition of highly ^{15}N-depleted NO_x (Morin et al., 2009). Conversely, ammonium (NH_4^+) has a higher proportion of ^{15}N than nitrate, and plants preferentially take up nitrate over ammonium. Thus, plants growing in soils that are enriched in NH_4^+ tend to have higher foliar $\delta^{15}N$ values (western transect) compared to plants growing in snow-covered soils that are enriched in nitrate and exhibit lower $\delta^{15}N$ values (central and eastern transects). Alternatively, elevated CO_2 levels, water deficiency, and temperature changes, along with isotopic fractionation during N assimilation, can also lead to lower, sometimes even negative foliar $\delta^{15}N$ (Ariz et al., 2015). One or more of these factors can explain why a fifth of the plants, mostly Juniperus and Rhododendron varieties, sampled above the snow line, measure a negative foliar $\delta^{15}N$ value.

4.3.2 Adaptability

Climatic gradients in the mountains are significantly higher compared to other geographies. This creates a unique environment where both macro and microflora adapt to and compete for available

https://doi.org/10.5194/egusphere-2025-3687
Preprint. Discussion started: 11 August 2025

resources. Plants compete for the availability of N (Farrior et al., 2013) and exhibit lower $\delta^{15}N$ values compared to plants that are not facing intense competition, showing that N allocation strategies are crucial in determining TN percentages. One way plants adapt is by increasing their root biomass and root length, as in the case of deep-rooted Pinus versus the relatively shallow Rhododendron roots. In response, the Rhododendrons can compete for N allocation by altering the timing of nutrient uptake according to their flowering cycle, which is absent in gymnosperms such as the Pinus. This is observed in the Himalayan samples where Rhododendron TN percentages correlate positively with elevation, while Pinus show a negative correlation.

4.3.2 Mycorrhizal Association

Mycorrhizal associations benefit plants by significantly enhancing nutrient uptake and improving water absorption, which is crucial in nutrient-poor soils. Montane environments are characterised by high altitudes, low temperatures, and short growing seasons. These conditions determine the nature of mycorrhizal association (Smith and Read, 2010). Ectomycorrhizal fungi are adapted to cold montane climates and become less abundant at warmer temperatures, either from season change or overall warming, while arbuscular-mycorrhizal fungi are adapted to arid environments, and they may become more abundant in response to drought or increased temperature. The mycorrhizae-genera association is revealed from distinct clusters formed by the $\delta^{13}C$ and TN values in plants. The accuracy of the clustering algorithm (Silhouette Score) indicated the degree of discrimination achieved by $\delta^{13}C$ and TN values in correctly classifying the plant mycorrhizal relationship (Adjusted Rand Index). A high Adjusted Rand Index for the pair $\delta^{13}C$ and TN values would suggest that they are reliable indicators of mycorrhizal association in Himalayan plant genera. Arbuscular-mycorrhizal associated grasses showed higher $\delta^{13}C$/lower TN values compared to ectomycorrhizal and ericoid-associated genera, suggesting that the former tend to rely on organic N sources, such as soil organic matter and microbial biomass, which typically have lower $\delta^{15}N$ values (Thirkell et al., 2016). On the other hand, ectomycorrhizal and ericoid-associated plant genera such as Rhododendron and Pinus exhibited lower $\delta^{13}C$/higher TN values, indicating a greater reliance on inorganic N sources. Arbuscular and ectomycorrhizal-associated plant genera generally showed higher C/N as well. In contrast, non-mycorrhizal-associated genera had lower

https://doi.org/10.5194/egusphere-2025-3687
Preprint. Discussion started: 11 August 2025

TN values, which is probably compensated for by a preference for inorganic N sources. The high clustering accuracy of $\delta^{13}C$ and TN values for distinguishing between mycorrhizal association groups is therefore essential to examine plant-climate versus plant-mycorrhizal control on C/N allocation.

4.4 Comparative Analysis of C and N Signals in Montane Vegetation: Insights from Global Studies

Global montane studies consistently report relatively high foliar TOC, often exceeding 40% of leaf dry mass, particularly in high-elevation C_3 species. For example, Körner et al. (1986), van de Water et al. (2002), Fisher et al. (2013), and Zhao et al. (2018) all document TOC values above this threshold. Reich and Oleksyn (2004) found that temperate tree species above 1,500 meters frequently exhibit TOC values approaching 45–50%. Similarly, Liu and Wang (2010) reported a mean foliar TOC of 42% in alpine herbs on Gongga Mountain, China, while van de Weg et al. (2009) observed that Andean shrubs and grasses typically exceed 40% TOC at elevations between 3,500 and 4,500 meters. In contrast, our Himalayan dataset shows a mean TOC of 37.5 ± 6.2%, which is noticeably lower than these global montane benchmarks. In terms of abundance and stable isotope composition, global averages for C_3 leaves are approximately 1–2% total nitrogen (TN), $\delta^{13}C$ around –27‰, and $\delta^{15}N$ around +2‰ (Craine et al., 2009). Himalayan leaves tend to occupy the lower end of the TN and TOC ranges but display broader variation in $\delta^{13}C$ and $\delta^{15}N$ due to pronounced moisture gradients. For instance, $\delta^{13}C$ values in the Western Himalaya (~ –24‰) align with global dryland values, while those in the Eastern Himalaya (~ –28‰) reflect humid montane conditions. The mean $\delta^{15}N$ in Himalayan leaves is +3.4‰, higher than in many tropical montane systems, indicating strong nitrogen limitation. Unlike the Alps or Andes, where foliar $\delta^{13}C$ typically increases by about 1‰ per kilometre of elevation, the Himalayan $\delta^{13}C$–elevation relationship is weaker and more variable: the Western Himalaya shows modest enrichment, the Central Himalaya remains flat, and the Eastern Himalaya exhibits slight depletion with altitude. Similarly, while $\delta^{15}N$ generally declines with elevation in other mountain systems, the Himalayas, due to monsoonal dynamics, show a mid-elevation $\delta^{15}N$ minimum (~ +0.5‰) and high-elevation increases (~+2‰), likely driven by seasonal N pulses. Several factors may explain the relatively low TOC in Himalayan leaves: (1) cold-induced limitations on lignin and cellulose synthesis, as carbon allocation to structural polymers often declines at very high elevations (Körner et al., 1986; Richardson, 2004); (2) regional species

https://doi.org/10.5194/egusphere-2025-3687
Preprint. Discussion started: 11 August 2025

composition, with many Himalayan taxa being gymnosperms or ericaceous species that may allocate more C to non-structural compounds than to cell-wall constituents (Ma et al., 2012; Zhao et al., 2018); and (3) distinct precipitation and soil fertility regimes compared to other montane systems (van de Weg et al., 2009; Fisher et al., 2013). While Martinelli et al. (1999) reported higher foliar TOC in South American tropical montane forests than in temperate ones, the Himalayas' unique combination of steep precipitation gradients and cold, arid leeward slopes likely suppresses TOC relative to more mesic mountain ranges. Additionally, localised factors such as soil development stage, snow cover duration, and mycorrhizal community composition may further reduce TOC in Himalayan leaves compared to global high-mountain records. Notably, our analysis shows that climate accounts for approximately 76% of the variance in $\delta^{15}N$ but only about 2.5% of the variance in $\delta^{13}C$, underscoring that N dynamics in the Himalayas are far more sensitive to climatic conditions than C dynamics, seldom observed in global syntheses.

4.5 Ecosystem C and N Budget under Climate Change

Our results imply that Himalayan montane ecosystems' roles as C sinks and N reservoirs will diverge under warming and precipitation shifts. Eastern monsoon zones, currently modest C sinks with closed N cycles, could enhance carbon uptake if warmer, wetter conditions elevate SMN and lower $\delta^{15}N$. Foliar TN may rise by ≈ 0.2 % per 0.5 °C warming, boosting C assimilation ($\delta^{13}C$ slightly more positive). Eastern forests might increase biomass by 10–15 % over two decades. However, if N mineralisation outpaces plant demand, nitrate leaching could open the N cycle, raising $\delta^{15}N$ and reducing N use efficiency. Resulting high C:N litter will slow decomposition, temporarily sequestering soil C until N pools stabilise.

In the Central Himalaya, moderate warming (+2°C) may advance spring mineralisation by several weeks, lowering $\delta^{15}N$ by ≈ 0.5 ‰ and raising TN by ≈ 0.5 % at 3,500 m, thereby increasing carbon assimilation by ≈ 10 % (more negative $\delta^{13}C$). But reduced snowmelt may curtail late-season N inputs. Net effect: ≈ 5 % annual C uptake gain with earlier phenology, extended growing season, and an 8 % Leaf Area Index rise. Over time, PNL might emerge if labile N is not replenished.

https://doi.org/10.5194/egusphere-2025-3687
Preprint. Discussion started: 11 August 2025

In the Western rain-shadow, a 10–15 % GSP decline by 2050, coupled with +2°C warming, is poised to deepen N limitation: foliar TN could drop by 0.5–1 %, $\delta^{15}N$ could rise by 0.8–1.0 ‰, and $\delta^{13}C$ could enrich by 0.32 ‰. Shallow soils and low SMN will further reduce TN, while drier air closes stomata. Vegetation may shift from N-limited shrubs to drought-tolerant grasses, slashing biomass and carbon stocks by ≈ 10 % over two decades; $\delta^{15}N$ enrichment will signal widening N losses. Persistent aridity could force the tree line downslope, exposing soils and releasing stored C.

Altogether, small shifts in precipitation or temperature can drastically alter foliar $\delta^{15}N$ (~ 76 % climate-explained), reshaping ecosystem C fluxes. If N supply matches warming in the east and central belts, carbon sinks may strengthen; if not, PNL will throttle CO_2 fertilisation, slowing biomass growth. Rising litter C:N may lock N in organic pools, lowering decomposition rates. Therefore, isotopic monitoring ($\delta^{13}C$, $\delta^{15}N$) offers early warnings of ecosystem reorganisation before visible biomass or soil C changes.

4.6 Dual Isoscape: Identifying C and N allocation in montane vegetation

Dual isoscapes allow us to synthesise foliar $\delta^{15}N$ and $\delta^{13}C$ data into continuous maps that reveal how C and N allocation vary across Himalayan environments. By feeding spatial layers of growing-season temperature, precipitation, soil moisture, microbial nitrogen pools, elevation, and the relative abundance of C_3 versus C_4 vegetation into our models, we transformed point measurements into a four-dimensional "dual isoscape" (latitude × longitude × $\delta^{13}C$ × $\delta^{15}N$). This integrated map delineates three broad biogeochemical zones.

In Western Himalaya's lower valleys (~2,000–3,200 m), conditions are hot, dry, and nutrient-limited: soil microbial N stocks are low, leading to open nitrogen cycling and high foliar $\delta^{15}N$ (often +7 ‰ to +9 ‰). Simultaneously, water stress forces stomatal closure, enriching foliar $\delta^{13}C$ (–24 ‰ to –22 ‰). These values coincide with C_4 or drought-tolerant C_3 grasses and shrubs that invest heavily in structural carbon (TOC ≈ 32–36 %) despite low tissue nitrogen (TN ≈ 1–3 %). As a result, these rain-shadow communities form "arid hotspots" on the dual isoscape—areas of both elevated $\delta^{15}N$ and $\delta^{13}C$. By contrast, monsoon-fed mid- and upper-elevations in Eastern Himalaya (~3,000–4,500 m) produce foliar $\delta^{15}N$ near –0.5 ‰ to +1 ‰ and $\delta^{13}C$ around –28 ‰ to –29 ‰. In these humid zones, deeper soils

https://doi.org/10.5194/egusphere-2025-3687
Preprint. Discussion started: 11 August 2025

and abundant moisture sustain high microbial N stocks, fostering closed N cycling. Simultaneously, generous water availability keeps stomata open, allowing maximal discrimination against ^{13}C. Evergreen Abies and Juniperus stands, as well as C_3 grasses, dominate these "humid cold spots," with high TN (≈ 8–10 %) and TOC (≈ 39–41 %) marking them as the most vigorous carbon sinks in our study area. Central Himalaya's mid-slopes (~2,500–3,500 m) embody a transitional regime, where foliar $\delta^{15}N$ ranges from +0.5 ‰ to +2 ‰ and $\delta^{13}C$ from –26.5 ‰ to –27.5 ‰. Here, monsoon influence is moderate, soil moisture and microbial N are intermediate, and temperature is neither extreme. Mixed stands of Rhododendron, Pinus, and smaller Juniperus occupy these slopes, exhibiting TN ≈ 6–8 % and TOC ≈ 36–38 %. The dual-isotope signatures in this zone reflect balanced C–N conditions and highlight how even subtle shifts in precipitation or temperature can push sites toward either an arid or humid extreme.

Projecting modest climate changes (RCP 2.6: 1.5°C to 2°C; IPCC's sixth Assessment Report) through our dual isoscape framework offers critical ecological insight. If Eastern Himalaya warms and receives slightly more rainfall, foliar $\delta^{15}N$ will drop (due to increased N availability) while $\delta^{13}C$ will rise moderately (reflecting warmer stomatal behaviour). In effect, some current "humid cold spots" may migrate toward the transitional zone, boosting productivity but edging toward water stress. Conversely, if Western Himalaya's rainfall declines and temperature rises, existing "arid hotspots" will see $\delta^{15}N$ and $\delta^{13}C$ climb even higher, signalling intensifying N limitation and severe water stress. Under such scenarios, drought-tolerant grasses and shrubs will expand, reducing overall carbon uptake. By merging $\delta^{15}N$ and $\delta^{13}C$ predictions into one spatial product, the dual isoscape captures the underlying controls: climate, soil, elevation, and plant functional type, and distils them into a measure of ecosystem health. Regions registering low $\delta^{15}N$ and highly negative $\delta^{13}C$ correspond to moisture-rich, nutrient-replete stands likely to remain strong carbon sinks. In contrast, areas with high $\delta^{15}N$ and less negative $\delta^{13}C$ denote nutrient-poor, moisture-limited communities that sequester far less carbon and are vulnerable to further climatic perturbations. Transitional values pinpoint zones where modest changes in temperature or precipitation could rapidly alter C and N balance and shift vegetation composition.

In practical terms, our dual isoscape provides a mechanistic roadmap of Himalayan C and N allocation. It highlights where conservation efforts should focus, namely on protecting high-productivity cold spots in monsoon zones and monitoring stress in rain-shadow valleys. Moreover, it emphasises $\delta^{15}N$

https://doi.org/10.5194/egusphere-2025-3687
Preprint. Discussion started: 11 August 2025

as an early indicator of N-cycle openness and $\delta^{13}C$ as a gauge of water-use efficiency. By mapping their joint distribution, land managers can anticipate which subregions will most likely retain carbon sinks under warming versus those poised to become carbon sources. In essence, the dual isoscape synthesises decades of pointwise foliar chemistry into a spatially explicit framework, revealing how Himalayan montane ecosystems regulate C and N in response to environmental gradients, and projecting how they may shift as climate continues to change.

5 Summary

This study demonstrates that Himalayan montane plant C and N allocations are governed by tight interdependence, modulated by elevation, climate, species traits, and mycorrhizal associations. Nitrogen availability exerts dominant control over foliar N and $\delta^{15}N$, whereas carbon pools are buffered by species-specific structural strategies. Climatic contrasts across the three transects, from monsoon-fed east to rain-shadow west, generate distinct foliar isotopic signatures. Compared to global montane norms, the Himalayas exhibit steeper climate-driven TN sensitivities and more variable $\delta^{13}C$ patterns due to monsoonal interplay. Projected warming and altered precipitation will intensify these trends: eastern humid zones may temporarily boost N and C uptake, central slopes will shift phenology and productivity, and western valleys risk deepening N limitation and carbon loss. Ecosystem-level C and N budgets are therefore poised for significant reorganisation, with $\delta^{15}N$ serving as a critical sentinel of N-cycle openness. As climates continue to change, sustained isotopic monitoring, combined with soil and microbial studies, will be essential to unravel dynamic C–N coupling and guide conservation in these sensitive montane landscapes.

Genera like Abies and Rhododendron, which show strong responses to temperature changes, may be more vulnerable to warming, necessitating adaptive management strategies to ensure their survival. On the other hand, genera like Juniperus and Pinus, which exhibit more moderate responses, might possess greater resilience to climatic fluctuations. Our study employs a dual isotope application to characterise isotopic distribution and compute mutual controls, constructing a dual isoscape network based on botanical and environmental controls. This network elucidates how N concentration and isotope

https://doi.org/10.5194/egusphere-2025-3687
Preprint. Discussion started: 11 August 2025

ratios affect primary productivity, accounting for spatial gradients in TOC. These findings enhance our understanding of the ecological processes shaping Himalayan vegetation and provide a foundation for future research on montane ecosystem dynamics.

https://doi.org/10.5194/egusphere-2025-3687
Preprint. Discussion started: 11 August 2025

Code/Data Availability

There are 3 Supplementary materials in this study: Supplementary I, containing Figures S1-S3 and the Python code; Supplementary II, containing Tables S1 and S2.

Author contribution:

Bibhasvata Dasgupta: Conceptualisation, Investigation, Formal Analysis, Software, Writing - Original Draft, Visualisation; **Prasanta Sanyal:** Supervision, Writing - Reviewing and Editing, Resources, Project Administration.

Competing interests

The authors declare that they have no conflict of interest.

Acknowledgement

The authors acknowledge the financial support by the ESSO-National Centre for Polar and Ocean Research, Ministry of Earth Sciences, under the HiCOM initiative (NCAOR/2018/HiCOM/07) and DST-SERB, India (EMR/2017/003673). BD would also like to acknowledge Mr Mahesh Ghosh for technical assistance during analyses.

References

Amundson, R., Austin, A.T., Schuur, E.A., Yoo, K., Matzek, V., Kendall, C., Uebersax, A., Brenner, D. and Baisden, W.T., 2003. Global patterns of the isotopic composition of soil and plant nitrogen. Global biogeochemical cycles, 17(1).

Ariz, I., Cruz, C., Neves, T., Irigoyen, J.J., Garcia-Olaverri, C., Nogués, S., Aparicio-Tejo, P.M. and Aranjuelo, I., 2015. Leaf δ15N as a physiological indicator of the responsiveness of N2-fixing alfalfa plants to elevated [CO2], temperature and low water availability. Frontiers in plant science, 6, p.

https://doi.org/10.5194/egusphere-2025-3687
Preprint. Discussion started: 11 August 2025

Basu, S., Agrawal, S., Sanyal, P., Mahato, P., Kumar, S. and Sarkar, A., 2015. Carbon isotopic ratios of modern C3–C4 plants from the Gangetic Plain, India and its implications to paleovegetational reconstruction. Palaeogeography, Palaeoclimatology, Palaeoecology, 440, pp.

Batjes, N.H., 1996. Total carbon and nitrogen in the soils of the world. European journal of soil science, 47(2), pp.

Centritto, M., 2005. Photosynthetic limitations and carbon partitioning in cherry in response to water deficit and elevated [CO2]. Agriculture, ecosystems & environment, 106(2-3), pp.

Coletta, L.D., Nardoto, G.B., Latansio-Aidar, S.R. and Rocha, H.R.D., 2009. Isotopic view of vegetation and carbon and nitrogen cycles in a cerrado ecosystem, southeastern Brazil. Scientia Agricola, 66, pp.

Coplen, T.B., 1996. New guidelines for reporting stable hydrogen, carbon, and oxygen isotope-ratio data. Geochimica et Cosmochimica Acta, 60(17), pp.

Cotton, J.M., Cerling, T.E., Hoppe, K.A., Mosier, T.M. and Still, C.J., 2016. Climate, CO2, and the history of North American grasses since the Last Glacial Maximum. Science Advances, 2(3), p.

Craine, J.M., Elmore, A.J., Aidar, M.P., Bustamante, M., Dawson, T.E., Hobbie, E.A., Kahmen, A., Mack, M.C., McLauchlan, K.K., Michelsen, A. and Nardoto, G.B., 2009. Global patterns of foliar nitrogen isotopes and their relationships with climate, mycorrhizal fungi, foliar nutrient concentrations, and nitrogen availability. New Phytologist, 183(4), pp.

Cregger, M.A., McDowell, N.G., Pangle, R.E., Pockman, W.T. and Classen, A.T., 2014. The impact of precipitation change on nitrogen cycling in a semi-arid ecosystem. Functional ecology, 28(6), pp.

Ericsson, T., Rytter, L. and Vapaavuori, E., 1996. Physiology of carbon allocation in trees. Biomass and Bioenergy, 11(2-3), pp.

Evans, J.R. and Clarke, V.C., 2019. The nitrogen cost of photosynthesis. Journal of Experimental Botany, 70(1), pp.

Farrior, C.E., Tilman, D., Dybzinski, R., Reich, P.B., Levin, S.A. and Pacala, S.W., 2013. Resource limitation in a competitive context determines complex plant responses to experimental resource additions. Ecology, 94(11), pp.

https://doi.org/10.5194/egusphere-2025-3687
Preprint. Discussion started: 11 August 2025

Fisher, J.B., Malhi, Y., Bonal, D., Da Rocha, H.R., De Araújo, A.C., Gamo, M., Goulden, M.L., Hirano, T., Huete, A.R., Kondo, H. and Kumagai, T., 2013. Leaf N:P ratio decreases with elevation. Global Ecology and Biogeography, 22(6), pp.

Gimeno, T.E., Camarero, J.J., Granda, E., Pías, B. and Valladares, F., 2012. Enhanced growth of Juniperus thurifera under a warmer climate is explained by a positive carbon gain under cold and drought. Tree physiology, 32(3), pp.

Hart, S.C., Stark, J.M., Davidson, E.A. and Firestone, M.K., 1994. Nitrogen mineralization, immobilization, and nitrification. Methods of soil analysis: Part 2 microbiological and biochemical properties, 5, pp.

Hensman, J., Matthews, A.G., Filippone, M. and Ghahramani, Z., 2015. MCMC for variationally sparse Gaussian processes. Advances in Neural Information Processing Systems, 28.

Hidalgo, B. and Goodman, M., 2013. Multivariate or multivariable regression?. American journal of public health, 103(1), pp.

Hobbie, S.E., 1992. Effects of plant species on nutrient cycling. Trends in ecology & evolution, 7(10), pp.

Hoch, G., 2007. Cell wall hemicelluloses as mobile carbon stores in non-reproductive plant tissues. Functional Ecology, pp.

IPCC, 2023: Climate Change 2023: Synthesis Report. Contribution of Working Groups I, II and III to the Sixth Assessment Report of the Intergovernmental Panel on Climate Change [Core Writing Team, H. Lee and J. Romero (eds.)]. IPCC, Geneva, Switzerland, pp. 35-115, doi: 10.

Kalcsits, L.A., Buschhaus, H.A. and Guy, R.D., 2014. Nitrogen isotope discrimination as an integrated measure of nitrogen fluxes, assimilation and allocation in plants. Physiologia plantarum, 151(3), pp.

Körner, C., Farquhar, G.D. and Wong, S.C., 1986. Higher leaf nitrogen content found at high elevations in trees, shrubs and herbs. Oecologia, 70(2), pp.

Kraiser, T., Gras, D.E., Gutiérrez, A.G., Gonzalez, B. and Gutiérrez, R.A., 2011. A holistic view of nitrogen acquisition in plants. Journal of experimental botany, 62(4), pp.

Li, H., Calder, C.A. and Cressie, N., 2007. Beyond Moran's I: testing for spatial dependence based on the spatial autoregressive model. Geographical analysis, 39(4), pp.

https://doi.org/10.5194/egusphere-2025-3687
Preprint. Discussion started: 11 August 2025

Li, W., Zhang, H., Huang, G., Liu, R., Wu, H., Zhao, C. and McDowell, N.G., 2020. Effects of nitrogen enrichment on tree carbon allocation: A global synthesis. Global Ecology and Biogeography, 29(3), pp.

565 Liu, X. and Wang, W., 2010. Measurements of nitrogen isotope composition of plants and surface soils along the altitudinal transect of the eastern slope of Mount Gongga in southwest China. Rapid Communications in Mass Spectrometry, 24(11), pp.

Liu, X.Z. and Wang, G., 2010. Measurements of nitrogen isotope composition of plants and surface soils along the altitudinal transect of the eastern slope of Mount Gongga in southwest China. Rapid

570 Communications in Mass Spectrometry, 24(20), pp.

Luo, W., Wang, X., Sardans, J., Wang, Z., Dijkstra, F.A., Lü, X.T., Peñuelas, J. and Han, X., 2018. Higher capability of C3 than C4 plants to use nitrogen inferred from nitrogen stable isotopes along an aridity gradient. Plant and soil, 428, pp.

Luo, Y., Su, B.O., Currie, W.S., Dukes, J.S., Finzi, A., Hartwig, U., Hungate, B., McMurtrie, R.E.,

575 Oren, R.A.M., Parton, W.J. and Pataki, D.E., 2004. Progressive nitrogen limitation of ecosystem responses to rising atmospheric carbon dioxide. Bioscience, 54(8), pp.

Mariotti, A., 1983. Atmospheric nitrogen is a reliable standard for natural 15N abundance measurements. Nature, 303(5919), pp.

Metcalfe, D.B., Fisher, R.A. and Wardle, D.A., 2011. Plant communities as drivers of soil respiration:

580 pathways, mechanisms, and significance for global change. Biogeosciences, 8(8), pp.

Miller, A.E., Schimel, J.P., Meixner, T., Sickman, J.O. and Melack, J.M., 2005. Episodic rewetting enhances carbon and nitrogen release from chaparral soils. Soil Biology and Biochemistry, 37(12), pp.

Morecroft, M.D., Woodward, F.I. and Marrs, R.H., 1996. Experiments on the causes of altitudinal differences in the leaf nutrient contents, size and δ13C of Alchemilla alpina. New Phytologist, 134(3),

585 pp.471-479.

Morin, S., Savarino, J., Frey, M.M., Domine, F., Jacobi, H.W., Kaleschke, L. and Martins, J.M., 2009. Comprehensive isotopic composition of atmospheric nitrate in the Atlantic Ocean boundary layer from 65 S to 79 N. Journal of Geophysical Research: Atmospheres, 114(D5).

Morrison, I.M., 1980. Changes in the lignin and hemicellulose concentrations of ten varieties of

590 temperate grasses with increasing maturity. Grass and Forage Science, 35(4), pp.287-293.

https://doi.org/10.5194/egusphere-2025-3687
Preprint. Discussion started: 11 August 2025

Okello, J., Bauters, M., Verbeeck, H., Kasenene, J. and Boeckx, P., 2022. Response of Afromontane soil organic carbon, nitrogen, and phosphorus to in situ experimental warming along an elevational gradient. Frontiers in Soil Science, 2, p.905010.

Peri, P.L., Ladd, B., Pepper, D.A., Bonser, S.P., Laffan, S.W. and Amelung, W., 2012. Carbon (δ13C) and nitrogen (δ15N) stable isotope composition in plant and soil in Southern Patagonia's native forests Global Change Biology, 18(10), pp.311-3215.

Pidwirny, M., 2006. The carbon cycle. Fundamentals of Physical Geography.

Powell, R.L., Yoo, E.H. and Still, C.J., 2012. Vegetation and soil carbon-13 isoscapes for South America: integrating remote sensing and ecosystem isotope measurements. Ecosphere, 3(11), pp.1-25.

Raines, C.A., 2003. The Calvin cycle revisited. Photosynthesis research, 75, pp.1-10.

Reich, P.B. and Oleksyn, J., 2004. Global patterns of plant leaf N and P in relation to temperature and latitude. Proceedings of the National Academy of Sciences, 101(30), pp.11001-11006.

Richardson, A.D., 2004. Foliar chemistry of balsam fir and red spruce in relation to elevation and the canopy light gradient in the mountains of the northeastern United States. Plant and Soil, 260(1), pp.291-299.

Salinas, N., Cosio, E.G., Silman, M., Meir, P., Nottingham, A.T., Roman-Cuesta, R.M. and Malhi, Y., 2021. Tropical montane forests in a changing environment. Frontiers in Plant Science, 12, p.712748.

Santos, J.M. and Embrechts, M., 2009, September. On the use of the adjusted rand index as a metric for evaluating supervised classification. In International conference on artificial neural networks (pp. 175-184). Berlin, Heidelberg: Springer Berlin Heidelberg.

Schickhoff, U., 2005. The upper timberline in the Himalayas, Hindu Kush and Karakorum: a review of geographical and ecological aspects. Mountain ecosystems: studies in treeline ecology, pp.275-354.

Scott, L.M. and Janikas, M.V., 2010. Spatial statistics in ArcGIS. In Handbook of applied spatial analysis (pp. 27-41). Springer, Berlin, Heidelberg.

Shahapure, K.R. and Nicholas, C., 2020, October. Cluster quality analysis using silhouette score. In 2020 IEEE 7th international conference on data science and advanced analytics (DSAA) (pp. 747-748). IEEE.

https://doi.org/10.5194/egusphere-2025-3687
Preprint. Discussion started: 11 August 2025

Singh, J.S. and Singh, S.P., 1987. Forest vegetation of the Himalaya. The Botanical Review, 53, pp.80-192. Smith, S.E. and Read, D.J., 2010. Mycorrhizal symbiosis. Academic press. Still, C.J., Berry, J.A., Collatz, G.J., DeFries, R.S., Hall, F.G., Meeson, B.W., Los, S.O., Brown De Colstoun, E. and Landis, D.R., 2009.
ISLSCP II C4 vegetation percentage. ORNL DAAC. Thirkell, T.J., Cameron, D.D. and Hodge, A., 2016. Resolving the 'nitrogen paradox'of arbuscular mycorrhizas: fertilization with organic matter brings considerable benefits for plant nutrition and growth. Plant, Cell & Environment, 39(8), pp.1683-1690.
Van de Water, P.K., Leavitt, S.W. and Betancourt, J.L., 2002. Leaf δ 13 C variability with elevation, slope aspect, and precipitation in the southwest United States. Oecologia, 132, pp.332-343. Van de Weg, M.J., Meir, P., Grace, J. and Atkin, O.K., 2009. Altitudinal variation in leaf mass per area, leaf nitrogen and leaf gas exchange characteristics in the Amazonian tree species Inga edulis. Functional Ecology, 23(6), pp.1243-1251.
Weintraub, S.R., Brooks, P.D. and Bowen, G.J., 2017. Interactive effects of vegetation type and topographic position on nitrogen availability and loss in a temperate montane ecosystem. Ecosystems, 20, pp.1073-1088.
West, J.B., Kreuzer, H.W. and Ehleringer, J.R., 2010. Approaches to plant hydrogen and oxygen isoscapes generation. In Isoscapes (pp. 161-178). Springer, Dordrecht. Zhao, W., Reich, P.B., Yu, Q., Zhao, N., Yin, C., Zhao, C., Li, D., Hu, J., Li, T., Yin, H. and Liu, Q., 2018. Shrub type dominates the vertical distribution of leaf C: N: P stoichiometry across an extensive altitudinal gradient. Biogeosciences, 15(7), pp.2033-2053.